Catalyst Characterization

DOI: 10.1002/ange.201311073

# Quantification of Zinc Atoms in a Surface Alloy on Copper in an Industrial-Type Methanol Synthesis Catalyst**

*Sebastian Kuld, Christian Conradsen, Poul Georg Moses, Ib Chorkendorff, and Jens Sehested**

***Abstract:*** *Methanol has recently attracted renewed interest because of its potential importance as a solar fuel.[1] Methanol is also an important bulk chemical that is most efficiently formed over the industrial $Cu/ZnO/Al_2O_3$ catalyst. The identity of the active site and, in particular, the role of ZnO as a promoter for this type of catalyst is still under intense debate.[2] Structural changes that are strongly dependent on the pretreatment method have now been observed for an industrial-type methanol synthesis catalyst. A combination of chemisorption, reaction, and spectroscopic techniques provides a consistent picture of surface alloying between copper and zinc. This analysis enables a reinterpretation of the methods that have been used for the determination of the Cu surface area and provides an opportunity to independently quantify the specific Cu and Zn areas. This method may also be applied to other systems where metal–support interactions are important, and this work generally addresses the role of the carrier and the nature of the interactions between carrier and metal in heterogeneous catalysts.*

It is widely accepted that the presence of ZnO increases the activity of copper-based systems towards methanol synthesis.[2a,3] Under reducing conditions, the presence of $ZnO_x$ species leads to partially covered Cu particles as a result of strong metal–support interactions (SMSI).[1a,4] Evidence for surface alloy formation has been obtained from studies of the deposition of metallic zinc on a copper single crystal and by ion-scattering measurements of a Cu/ZnO catalyst with isotopically enriched Cu and Zn.[5] In a previous study, a change in the copper area was observed subsequent to pretreatments in reducing atmospheres by combining $N_2O$ reactive frontal chromatography ($N_2O$-RFC) and temperature-programmed desorption of $H_2$ ($H_2$-TPD).[6] Studies of Cu/ZnO model systems have revealed that pretreatments influence the morphology of Cu nanoparticles by wetting/non-wetting, which was explained by the formation of strongly binding oxygen vacancies at the ZnO surface.[4a,b,7] Most recently, ambient-pressure X-ray photoelectron spectroscopy (XPS) of Cu/ZnO catalysts with a high Cu content has shown that surface decoration of Cu nanoparticles with $ZnO_x$ species occurs under relatively mild conditions.[2a,b] It was suggested that the active site consists of Cu steps that are decorated with Zn atoms and stabilized by bulk defects.[2a,c]

Herein, the nature of the SMSI between $ZnO_x$ and Cu under reducing conditions is investigated for an industrial-type methanol catalyst. A systematic examination using several methods has shown significant dynamical changes in the state of the copper surface as a consequence of an increasing partial pressure of hydrogen. This study elucidates the pitfalls of chemisorption methods for determining the Cu surface area and offer a more accurate determination of the specific Cu surface area together with strong evidence that Zn is present in its metallic state in a Cu/Zn surface alloy. Surface-sensitive methods provide information on the specific copper and zinc areas as a function of the partial pressure of hydrogen during the pretreatment. Furthermore, these methods provide quantitative information on the Zn oxidation state and the coverage of the Cu surfaces.

An industrial-type $Cu/ZnO/Al_2O_3$ catalyst was subjected to two experimental sequences in a combined HPC (high pressure cell) and UHV (ultra-high vacuum) setup and in a fixed-bed reactor system, respectively (Figure 1). In both systems, pretreatment of the catalyst consisted of a reduction in a $H_2$/He gas mixture. The temperature was increased by 2 K min$^{-1}$ from 300 to 493 K, which was followed by a 16 h dwell time at 493 K where the catalyst was exposed to different partial pressures of hydrogen.

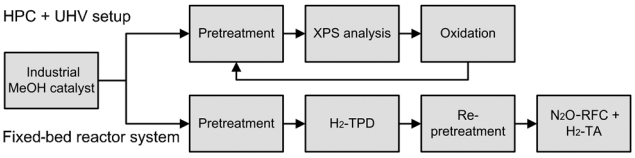


***Figure 1.*** Block diagram of the experimental treatment sequences that were applied in this work. The upper route was used for the combined HPC and UHV system, whereas the bottom sequence was used for a fixed-bed reactor system.

In the combined HPC and UHV system, the $Cu/ZnO/Al_2O_3$ catalyst and pure ZnO powder (Transpek-Silox Industry) were tabletized and placed in a custom-made stainless-steel sample holder. Before characterization and pretreatment, the catalyst tablet was kept under UHV and heated to

[*] S. Kuld,[+] Dr. P. G. Moses, Dr. J. Sehested
Haldor Topsøe Research Laboratories
Nymøllevej 55, 2800 Kgs. Lyngby (Denmark)
E-mail: jss@topsoe.dk
C. Conradsen,[+] Prof. I. Chorkendorff
CINF, Department of Physics, Technical University of Denmark
Building 312, 2800 Kgs. Lyngby (Denmark)
[+] These authors contributed equally to this work.

[**] For funding of this work, we gratefully acknowledge The Danish National Research Foundation's Center for Individual Nanoparticle Functionality (DNRF54). We thank Stig Helveg for his comments on the manuscript.

Supporting information for this article is available on the WWW under http://dx.doi.org/10.1002/anie.201311073.

  

120 °C for two hours to remove water. After initial XPS, the catalyst was transferred to the HPC and exposed to the pretreatment. The surface was reset by heating the sample to 70 °C in an $O_2$/Ar atmosphere (5000 ppm) for 16 hours between the pretreatments.

The XPS characterization after the pretreatment was conducted to examine the extent to which metallic Zn is present in the catalyst (Supporting Information, Figure S1). It is not trivial to detect the reduction of ZnO to Zn by XPS. The Zn $2p_{3/2}$ lines for Zn and ZnO are positioned at 1021.4 eV and 1021.7 eV, respectively.[8] The change in the valence state from $Zn^{II}$ to $Zn^0$ was observed as a more pronounced 3 eV downward shift of the binding energy of the Zn $L_3M_{4.5}M_{4.5}$ Auger peak (Zn Auger; Figure S2b). In Figure 2a, the Zn Auger peak is shown for the $Cu/ZnO/Al_2O_3$ catalyst after pretreatment with hydrogen pressures of 0.01–1 bar. In Figure 2b, the Zn Auger lines for the pure ZnO reference and the $Cu/ZnO/Al_2O_3$ system before and after pretreatment at 1 bar $H_2$ are displayed. The positions of all Auger peaks were aligned by the C1s peak, and a Shirley background was subtracted. The Zn Auger peak from $Cu/ZnO/Al_2O_3$ in Figure 2b is normalized to the peak height of the ZnO Auger feature. The Zn Auger spectrum shown in Figure 2 consists of a multiplex of many lines,[9] but only the changes that are due to reduction were considered. In the Zn Auger spectrum of the $Cu/ZnO/Al_2O_3$ catalyst that was recorded after pretreatment under hydrogen atmosphere (0.01 bar), a shoulder feature appeared at a binding energy that was reduced by 3 eV (Figure 2a). The shoulder feature becomes more pronounced for higher partial pressures of hydrogen. When the pure ZnO tablet was reduced at 1 bar $H_2$ for 16 hours, no change of the Auger peak was observed (Figure 2b), which is in clear contrast to the results that were obtained with the $Cu/ZnO/Al_2O_3$ catalyst.

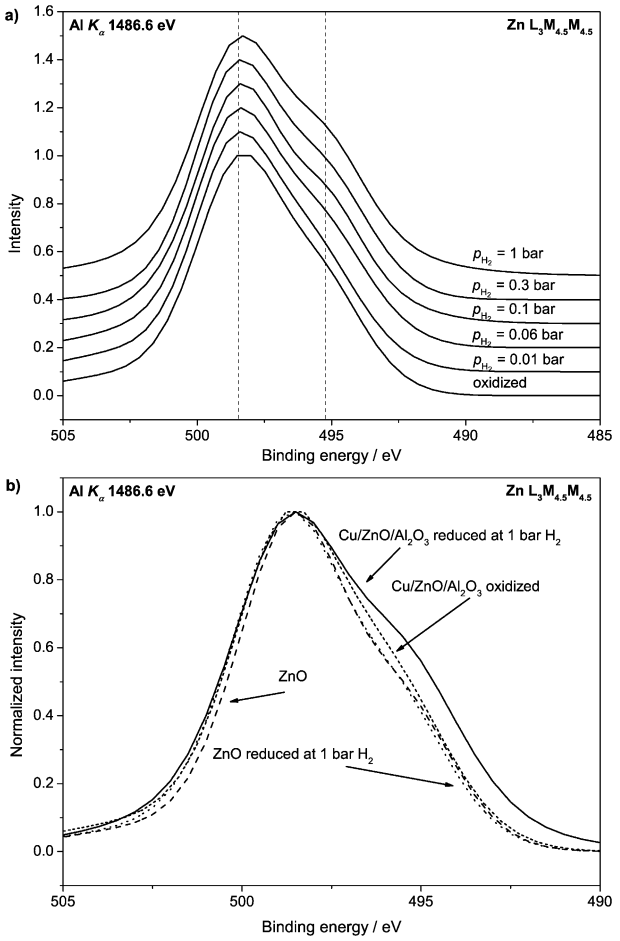


***Figure 2.*** a) The Zn $L_3M_{4.5}M_{4.5}$ Auger peaks for the oxidized and reduced $Cu/ZnO/Al_2O_3$ catalyst. b) Reference spectra of pure ZnO, reduced ZnO, and the $Cu/ZnO/Al_2O_3$ catalyst both in its oxidized and reduced form.

Analysis of the Cu $L_3VV$ Auger peak shows that the Cu nanoparticles are reduced to the metallic state after each pretreatment (Figure S2). The O1s XPS peak showed no change when the hydrogen partial pressure was varied during the pretreatment (Figure S3).

The Auger peaks in Figure 2 were fitted as a linear combination of the oxidized Auger peak, and the oxidized Auger peak shifted downwards by 3 eV in binding energy. According to the literature, the changes in the shoulder feature of the Zn Auger line could originate from both oxygen vacancies in ZnO thin films and metallic Zn in brass.[10] The existence of oxygen vacancies was reflected by a shake-up feature of the O1s peak by a 1.3 eV shift. As the O1s XPS peak was unaffected by the pretreatment, the Auger shoulder feature may be attributed to metallic Zn. Therefore, a deconvolution of the fit can be used to quantify the amount of metallic Zn and ZnO (Figure S4a). In Figure 3a, the changes in the peak areas of Zn and ZnO are shown for different pretreatment conditions for both the $Cu/ZnO/Al_2O_3$ catalyst and the pure ZnO reference sample. A gradual enrichment with metallic Zn of up to 10% was observed for the $Cu/ZnO/Al_2O_3$ catalyst subsequent to the pretreatment. When the ZnO reference sample was exposed to 1 bar of $H_2$, metallic Zn was not observed. These measurements demonstrate the importance of copper in industrial-type catalysts for catalyzing the reduction of ZnO.

In the fixed-bed reactor system, two-step series of experiments were applied for each set of pretreatment conditions. First, the Cu area was determined by $H_2$-TPD (Figure S5) subsequent to the pretreatment. $H_2$-TPD is known to be nondestructive with respect to the Cu surface area.[11] Second, a re-pretreatment was followed by $N_2O$-RFC at 50 °C[12] (Figure S6) and finally $H_2$ transient adsorption ($H_2$-TA) measurement using 1% $H_2$/He at room temperature (Figure S7). The re-pretreatment was carried out to ensure that the $N_2O$-RFC was conducted on an adsorbate-free reduced Cu surface. After each series of experiments, the catalyst sample was replaced.

The Cu areas that were measured for the $Cu/ZnO/Al_2O_3$ catalyst after pretreatment with different partial pressures of hydrogen are shown in Figure 3b. The Cu area was determined by $H_2$-TPD, $N_2O$-RFC, and $H_2$-TA methods and was measured as the area of the Cu surface per catalyst weight. After pretreatment with 0.01 bar of hydrogen, the $N_2O$ titration method and $H_2$-TPD essentially gave the same Cu area of approximately 16.5 $m^2 g^{-1}$. $H_2$-TA gave a slightly lower

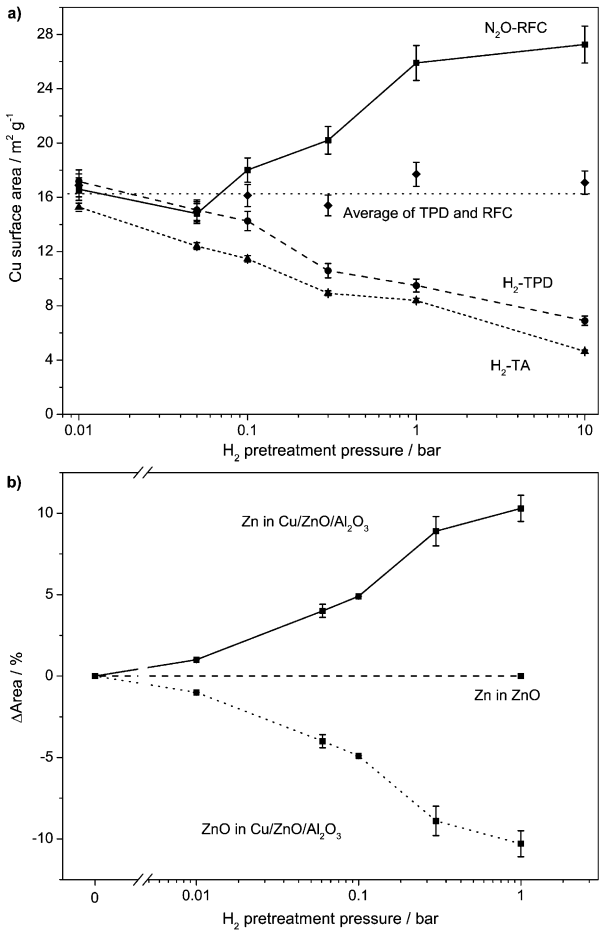


***Figure 3.*** a) The change in the area of the ZnO (-----) and Zn (——) Auger peaks for the industrial-type $Cu/ZnO/Al_2O_3$ catalyst and the change in the area for the ZnO reference sample (– – –). b) The change in the Cu surface area as determined by $N_2O$-RFC (■, ——), $H_2$-TPD (●, – – –), and $H_2$-TA (▲, •••••) after pretreatment at different partial pressures of $H_2$ for 16 hours. For $N_2O$-RFC and $H_2$-TA, the error bars are the relative differences between two identical experiments. The error bars for $H_2$-TPD are 5%, as discussed in the Supporting Information. The average of the Cu areas as determined by $H_2$-TPD and $N_2O$-RFC is indicated by ◆. The horizontal dotted line is to guide the eye.

area (−13%). This is ascribed to incomplete reduction of $Cu_2O$ (see the Supporting Information for details). The Cu area determined by $N_2O$-RFC was observed to increase with the partial pressure of hydrogen in the pretreatment above 0.05 bar. The surface area of the same catalyst, as determined by $H_2$-TPD and $H_2$-TA, decreases as a function of the hydrogen partial pressure. Despite the relatively low temperature during the pretreatment, the impact of the hydrogen partial pressure on the surface area as determined by the three different methods varies substantially, that is, up to ±60–65%. The average of the surface area based on the $N_2O$-RFC and $H_2$-TPD measurements displayed in Figure 3b (◆) is approximately constant and independent of the pretreatment.

Previous STM studies of Zn deposition on Cu(111) single crystals have shown that a Cu/Zn surface alloy can be formed by the random and homogeneous substitution of Zn atoms into the Cu(111) surface layer.[5a,b] The XPS data presented is in agreement with the formation of a Cu/Zn surface alloy. The shoulder feature of the Zn Auger line, which corresponds to metallic Zn, provides strong evidence for the reduction of ZnO to metallic Zn at the interface between the Cu and ZnO particles. The formation of a Cu/Zn surface alloy is also supported by the data that is shown in Figure 3b (see below).

The measurements of the Cu surface area by $N_2O$-RFC and $H_2$-TPD deviate to an increasing extent as the partial pressure of $H_2$ is raised during the pretreatment (Figure 3b). The determination of the Cu area by $N_2O$-RFC relies on the assumption that only Cu is present in the metallic state, that is, Cu is the only element that is responsible for the oxygen adsorption during $N_2O$ decomposition. However, the oxidation process is not selective in nature. As indicated by XPS, the incorporation of reduced zinc atoms into the surface of the copper nanoparticles will increase the oxygen uptake from $N_2O$ as each Zn atom that has been incorporated into the Cu surface is expected to react with one $N_2O$ molecule, whereas one surface Cu atom only reacts with 0.5 $N_2O$ molecules.

In contrast to the $N_2O$-RFC measurement, the $H_2$-TPD peak decreases with an increase in hydrogen partial pressure during the pretreatment. The $H_2$-TPD method is based on the specific desorption profile that is associated with metallic Cu only. Therefore, the incorporation of reduced Zn at the surface of the Cu particles leads to a decrease in the Cu area that is measured by the $H_2$-TPD method. Density functional theory (DFT) calculations show that the hydrogen adsorption energy at Zn sites that are incorporated into a Cu(111) surface will decrease by 28 kJ mol$^{-1}$ compared to that at a clean Cu(111) surface (Table S1). This implies that if Zn forms a surface alloy with Cu, a reduction in the peak area that is obtained by the $H_2$-TPD measurement can be directly related to a decrease in the Cu surface area and to the incorporation of Zn into the surface of the Cu particles.

The formation of a Cu/Zn surface alloy is supported by a comparison of the XPS data and the Cu areas determined by $H_2$-TPD. The comparison is based on a simple geometric model and uses the fraction of reduced and oxidized Zn atoms to calculate the loss of Cu surface atoms (Figure S10). In Figure 4a, the specific Cu surface area that was calculated from the XPS data as a function of the pretreatment $H_2$ pressure is compared to the $H_2$-TPD data, assuming that the latter only probes the Cu surface atoms. Figure 4a shows a clear correlation between the amount of metallic Zn measured by XPS and the decrease in the Cu surface area that was determined by $H_2$-TPD, which corroborates the hypothesis that $H_2$-TPD is an accurate method for determining the specific Cu (Zn-free) surface area.

The Cu surface area derived from the $H_2$-TA experiment was calculated by assuming that water is formed during the reduction of oxygen that is chemisorbed at the Cu surface (Figure S6).[13] Despite the fact that the area determined by $N_2O$-RFC increases with the pretreatment pressure, the amount of $H_2$ that is consumed in the $H_2$-TA experiment decreases in the same manner as for the $H_2$-TPD experiment. This observation is very reasonable in the context of Cu/Zn surface alloy formation. The Zn enrichment in the Cu surface

  

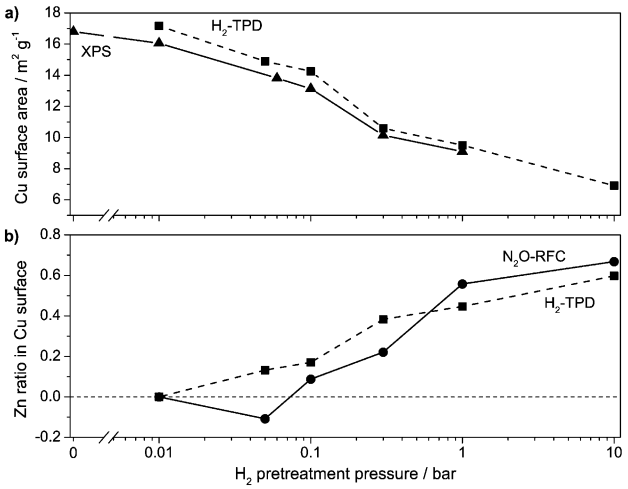


***Figure 4.*** a) Correlation between the Cu surface areas that were determined by $H_2$-TPD (■) and that are based on the XPS data (▲) by applying a simple model. b) The ratio of Zn enrichment in the Cu surface was evaluated for both the $N_2O$-RFC (●) and $H_2$-TPD (■) techniques.

layer leads to the formation of ZnO during $N_2O$-RFC. The less reducible nature of ZnO prohibits $H_2$ consumption during the $H_2$-TA experiment. The $H_2$-TA experiment probes the amount of oxygen in the $Cu_2O$ surface layer that is formed during the $N_2O$-RFC experiment, but not the amount of ZnO in the Cu surface (Figure S8).

The interaction between ZnO and Cu under reducing conditions has often been interpreted as a $ZnO_x$ layer on the Cu surface.[1a,4] Herein, we provide strong evidence that the identity of this layer is a Cu/Zn alloy. First, the position of the shoulder of the Zn Auger peak agrees well with that for reduced Zn in Cu, and the fact that the O 1s line is unaffected by reduction seems to exclude formation of a $ZnO_x$ layer. Second, the results from the different techniques, that is, XPS, $H_2$-TPD, $N_2O$-RFC, and $H_2$-TA, corresponds to those expected for a Cu/Zn surface alloy. This agreement is highly unlikely in the case of a $ZnO_x$ layer on top of the Cu particles. In situ TEM studies have not provided evidence for the formation of a $ZnO_x$ layer on the Cu surfaces under reducing conditions,[4b,7a] whereas a study that combined in situ TEM and electron energy loss spectroscopy (EELS) provided evidence for Cu/Zn alloy formation in a Cu/ZnO catalyst under $CO/H_2$ atmosphere.[14] We therefore conclude that the results presented here provide strong evidence for the formation of a Cu/Zn surface alloy.

Based on this conclusion, the data in Figure 3b enables a quantification of the amount of metallic Zn in the Cu/Zn surface alloy. The relative change in the surface area that was measured after pretreatment at 10 mbar $H_2$ is interpreted as a change in the Zn/Cu element ratio in the surface of the Cu particles. In Figure 4b, the amount of Zn in the Cu surface was calculated from the $H_2$-TPD and the $N_2O$-RFC experiment, respectively. The Zn enrichment in the Cu surface layer as a function of the pretreatment was seen to be similar even though two independent techniques were applied. The Zn enrichment in the Cu surface layer reached approximately 60% for a pretreatment of 16 hours at 10 bar $H_2$. This observation is remarkable taking into account the relatively mild conditions that were applied during the pretreatment. Another interesting observation is that the average surface area measured by $N_2O$-RFC and $H_2$-TPD is approximately independent of the pretreatment hydrogen pressure (see Figure 3b). This indicates that the total geometric surface area of the Cu particles is virtually unchanged during the reduction process, perhaps because wetting of Cu and ZnO particles of a similar size does not significantly change the exposed Cu surface area.

In conclusion, a study that combined XPS, $H_2$-TPD, $N_2O$-RFC, and $H_2$-TA measurements has provided clear evidence for an incorporation of metallic Zn atoms into the surface of Cu particles. Merging the results of these measurements gives insight into the debated origin of surface $ZnO_x$ species. XPS revealed an enhancement of the metallic Zn feature in the Zn Auger peak with an increase in the partial pressure of $H_2$. The presence of copper particles is found to be essential for the reduction of ZnO. These experimental observations are consistent with the formation of a Cu/Zn surface alloy during pretreatment. The interplay between the surface areas that were evaluated using $N_2O$-RFC and $H_2$-TPD methods can be utilized to quantify the amount of metallic Zn in the Cu surface. The $N_2O$-RFC method has previously been used several times to determine the Cu surface area.[15] This study provides a reinterpretation and a more accurate determination of the specific Cu surface, which is based on specific area measurements using four independent and consistent methods. Similar methods may be used for other metal–oxide systems where reduction of the oxide takes place. The presence of Zn atoms in a Cu surface has been shown experimentally to enhance the activity of a Cu surface,[16] and more recently, this has also been justified theoretically.[2a] We have now presented evidence that a surface alloy of Zn and Cu can be formed in industrial-type methanol synthesis catalysts under relatively mild conditions. These results support the idea that the presence of Zn atoms in the surface of Cu particles is important for increasing the activity of the Cu surface of a Cu/ZnO-based methanol synthesis catalyst.

## *Experimental Section*

Measurements of the specific Cu areas were carried out in a fixed-bed flow setup. The system consisted of a gas-delivering system, a U-shaped reactor unit, and a gas analyzer, as previously described.[11,17] Gases of high purity were used: He (99.9999%), $H_2$ (99.9999%), $H_2$/He (1% $H_2$, 99.9995%), $N_2O$/He (1% $N_2O$, 99.9995%). Fast online gas analysis was performed by a calibrated quadrupole mass spectrometer (Balzers GAM 445).

The $Cu/ZnO/Al_2O_3$ catalyst that was used for the present experiments was an industrial-type $Cu/ZnO/Al_2O_3$ catalyst (60:25:15; mol%) made by a co-precipitation method that is similar to a previously described procedure.[18] A large sample of the catalyst was aged in dry synthesis gas ($CO/CO_2/H_2 = 5:5:90$) at 250°C for 72 hours at very low space velocity and passivated in dilute oxygen. Samples of this catalyst were used in the present work. For each experiment, 200 mg of the aged catalyst with a sieve fraction of 150–300 μm were loaded into the U-shaped quartz reactor with an inner diameter of 4 mm. To determine the copper surface area, the procedure for $H_2$-TPD experiments that was described by Muhler

  

et al. was followed.[11] The copper surface area was equivalently determined by $N_2O$-RFC as reported by Chinchen et al.[12]

The XPS measurements were performed in a UHV setup with a base pressure of $10^{-10}$ Torr. The catalyst could be transferred to an HPC for pretreatment. The pressure in the HPC was controlled by a pressure controller to be 1 bar, and the gas flow of He and $H_2$ or oxygen was controlled by mass flow controllers. For the XPS measurements, the X-rays were generated from a dual-anode X-ray source from SPECS using Al $K_\alpha$ radiation with a photon energy of 1486.6 eV, whereas the photoelectrons were measured with a Phoibos Hemispherical Energy Analyzer.

Received: December 20, 2013
Revised: March 3, 2014
Published online: April 24, 2014

**Keywords:** catalysis · copper/zinc alloys · metal–support interactions · methanol · surface chemistry

[1] a) G. A. Olah, *Angew. Chem.* **2013**, *125*, 112 – 116; *Angew. Chem. Int. Ed.* **2013**, *52*, 104 – 107; b) G. A. Olah, *Chem. Eng. News* **2003**, *81* (36), 42 – 42.

[2] a) M. Behrens, F. Studt, I. Kasatkin, S. Kühl, M. Hävecker, F. Abild-Pedersen, S. Zander, F. Girgsdies, P. Kurr, B. L. Kniep, M. Tovar, R. W. Fischer, J. K. Nørskov, R. Schlögl, *Science* **2012**, *336*, 893 – 897; b) S. Zander, E. L. Kunkes, M. E. Schuster, J. Schumann, G. Weinberg, D. Teschner, N. Jacobsen, R. Schlögl, M. Behrens, *Angew. Chem.* **2013**, *125*, 6664 – 6669; *Angew. Chem. Int. Ed.* **2013**, *52*, 6536 – 6540; c) T. Kandemir, F. Girgsdies, T. C. Hansen, K. D. Liss, I. Kasatkin, E. L. Kunkes, G. Wowsnick, N. Jacobsen, R. Schlögl, M. Behrens, *Angew. Chem.* **2013**, *125*, 5271 – 5276; *Angew. Chem. Int. Ed.* **2013**, *52*, 5166 – 5170; d) J. B. Hansen, P. E. H. Nielsen in *Handbook of Heterogeneous Catalysis*, *Vol. 6*, 2nd ed. (Eds.: G. Ertl, G. Knözinger, F. Schüth, J. Weitkamp), Wiley-VCH, Weinheim, **2008**, pp. 2920 – 2949.

[3] M. Kurtz, N. Bauer, H. Wilmer, O. Hinrichsen, M. Muhler, *Chem. Eng. Technol.* **2004**, *27*, 1146 – 1150.

[4] a) J. D. Grunwaldt, A. M. Molenbroek, N. Y. Topsøe, H. Topsøe, B. S. Clausen, *J. Catal.* **2000**, *194*, 452 – 460; b) P. L. Hansen, J. B. Wagner, S. Helveg, J. R. Rostrup-Nielsen, B. S. Clausen, H. Topsøe, *Science* **2002**, *5562*, 2053 – 2055; c) R. Naumann d'Alnoncourt, X. Xia, J. Strunk, E. Löffler, O. Hinrichsen, M. Muhler, *Phys. Chem. Chem. Phys.* **2006**, *8*, 1525 – 1538; d) Y. Kanai, T. Watanabe, T. Fujitani, M. Saito, J. Nakamura, T. Uchijima, *Catal. Lett.* **1994**, *27*, 67 – 78; e) N. Y. Topsøe, H. Topsøe, *Top. Catal.* **1999**, *8*, 267 – 270; f) E. D. Batyrev, J. C. van den Heuvel, J. Beckers, W. P. A. Jansen, H. L. Castrium, *J. Catal.* **2005**, *229*, 136 – 142.

[5] a) M. Sano, T. Adaniya, T. Fujitani, J. Nakamura, *J. Phys. Chem. B* **2002**, *106*, 7627 – 7633; b) M. Sano, T. Adaniya, T. Fujitani, J. Nakamura, *Surf. Sci.* **2002**, *514*, 261 – 266; c) M. M. Viitanen, W. P. A. Jansen, R. G. Van Welzenis, H. H. Brongersma, *J. Phys. Chem. B* **1999**, *103*, 6025 – 6029; d) W. P. A. Jansen, J. Beckers, J. C. v. d. Heuvel, A. W. Denier van der Gon, A. Bliek, H. H. Brongersma, *J. Catal* **2002**, *210*, 229 – 236.

[6] H. Wilmer, O. Hinrichsen, *Catal. Lett.* **2002**, *82*, 117 – 122.

[7] a) P. C. K. Vesborg, I. Chorkendorff, I. Knudsen, O. Balmes, J. Nerlov, A. M. Molenbroek, B. S. Clausen, S. Helveg, *J. Catal.* **2009**, *262*, 65 – 72; b) C. V. Ovesen, B. S. Clausen, J. Schiøtz, P. Stoltze, H. Topsøe, J. K. Nørskov, *J. Catal.* **1997**, *168*, 133 – 142.

[8] Y. K. Gao, F. Traeger, O. Shekhah, H. Idriss, C. Wöll, *J. Colloid Interface Sci.* **2009**, *338*, 16 – 21.

[9] S. Aksela, J. Väyrynen, H. Aksela, *Phys. Rev. Lett.* **1974**, *33*, 999 – 1002.

[10] a) S. Ullah Awan, S. K. Hasanain, M. F. Bertino, G. H. Jaffari, *J. Appl. Phys.* **2012**, *112*, 103924; b) V. Schott, H. Oberhofer, A. Birkner, M. Xu, Y. Wang, M. Muhler, K. Reuter, C. Wöll, *Angew. Chem.* **2013**, *125*, 12143 – 12147; *Angew. Chem. Int. Ed.* **2013**, *52*, 11925 – 11929.

[11] M. Muhler, L. P. Nielsen, E. Törnqvist, B. S. Clausen, H. Topsøe, *Catal. Lett.* **1992**, *14*, 241.

[12] G. C. Chinchen, C. M. Hay, H. D. Vendervell, K. C. Waugh, *J. Catal.* **1987**, *79*, 103.

[13] O. Hinrichsen, T. Genger, M. Muhler, *Stud. Surf. Sci. Catal.* **2000**, *130*, 3825 – 3830.

[14] J. B. Wagner, P. L. Hansen, A. M. Molenbroek, H. Topsøe, B. S. Clausen, S. Helveg, *J. Phys. Chem. B* **2003**, *107*, 7753 – 7758.

[15] G. Prieto, J. Zecevic, H. Friedrich, K. P. de Jong, P. E. de Jong, *Nat. Mater.* **2013**, *12*, 34 – 39.

[16] J. Nakamura, I. Nakamura, T. Uchijima, T. Watanaba, T. Fujitani, *Stud. Surf. Sci. Catal.* **1996**, *101*, 1389 – 1399.

[17] T. Genger, O. Hinrichsen, M. Muhler, *Catal. Lett.* **1999**, *59*, 137.

[18] C. Baltes, S. Vukojevic, F. Schüth, *J. Catal.* **2008**, *258*, 334 – 344.

  